drones

MDPI

Article

Files Cooperative Caching Strategy Based on Physical Layer Security for Air-to-Ground Integrated IoV

Weiguang Wang [1,2], Hui Li [1,*], Yang Liu [1], Wei Cheng [1] and Rui Liang [1]

[1] School of Electronics and Information, Northwestern Polytechnical University, Xi'an 710129, China
[2] Department of Computer Science, University of Victoria, Victoria, BC V8P 5C2, Canada
* Correspondence: lh@nwpu.edu.cn

Abstract: Mobile edge cache (MEC)-enabled air-to-ground integrated Internet of Vehicles (IoV) technology can solve wireless network backhaul congestion and high latency, but security problems such as eavesdropping are often ignored when designing cache strategies. In this paper, we propose a joint design of cache strategy and physical layer transmission to improve the security offloading ratio of MEC-enabled air-to-ground IoV. By using the random geometry theory and Laplace transform, we derive the closed-form expression of the network security offloading ratio, which is defined as the probability that the request vehicle (RV) successfully finds the required file around it and obtains the file with a data rate larger than a given threshold. During the file acquisition process, we collectively consider the impact of the successful connection and secure transmission in the vehicle wireless communication. Then, we establish an optimization problem for maximizing the network security offloading ratio, in which the cache strategy and the secure transmission rate are jointly optimized. Furthermore, we propose an alternating optimization algorithm to solve the joint optimization problem. Simulation experiments verify the correctness of our theoretical derivation, and prove that the proposed cache strategy is superior to other existing cache strategies.

Keywords: air-ground collaborative IoV; vehicle-to-vehicle (V2V); caching strategy; the secure transmission rate; physical layer security (PLC)

Citation: Wang, W.; Li, H.; Liu, Y.; Cheng, W.; Liang, R. Files Cooperative Caching Strategy Based on Physical Layer Security for Air-to-Ground Integrated IoV. *Drones* **2023**, *7*, 163. https://doi.org/10.3390/drones7030163

Academic Editor: Vishal Sharma

Received: 9 January 2023
Revised: 23 February 2023
Accepted: 23 February 2023
Published: 26 February 2023

1. Introduction

According to Cisco's 2018–2023 Internet Annual Report, global devices and connected devices will grow at a compound annual growth rate (CAGR) of 10%, and IoV-based applications will grow at a CAGR of 17% [1,2]. The explosive growth of mobile data will bring a heavy burden to the core network. Currently, if a proper solution is not found to address the explosive growth of data traffic, it may degrade the quality experience of user vehicle (UV) and even cause congestion on backhaul links in the future. However, the present technologies can not meet all requirements in fifth generation communication network (5G), and there will be higher requirements for wireless network latency, coverage, spectrum and energy efficiency [3–7] in sixth generation communication network (6G). In order to satisfy the above requirements, 6G will need a paradigm shift to provide intelligent services for mobile devices. MEC-enabled air-to-ground integrated IoV technology has been proven to be a key technology in vehicle wireless networks, which can fully utilize the cache space of edge UV to improve network resiliency, reduce latency, and backhaul traffic [8–11]. Vehicle-to-Vehicle (V2V) communication can allow UV to directly share files to other UV around without going through the core network. The previous theoretical and practical research on mobile edge cache (MEC) based on V2V communication shows that V2V communication technology can effectively improve the throughput of IoV [12–14]. Therefore, MEC-enabled air-to-ground integrated IoV technology will have better application prospects in the 6G wireless communication network.

By utilizing the V2V communication technology, the adjacent UVs with MEC capability can communicate with each other directly without relying on the data forwarding of the

air base station (ABS), which will further improve the quality of service (QoS) of UVs and network performance. Since the cache capacity of the UV is also limited, it is necessary to design an optimal caching strategy to reasonably cache content to maximize network utility. Most of the existing caching strategy research use hit ratio, energy efficiency (EE), and network delay as optimization indicators. The significant breakthroughs have been made in these research directions [15–22]. Dai et al. [15] proposed a cooperative caching-multicast strategy based on V2V communication technology to improve the timeliness and spatial coverage of content services. They analyzed and verified the effectiveness of the strategy through the main technical indicators of average transmission coverage and average transmission delay. In order to obtain a more accurate caching strategy, Ning et al. [16] considered the effects of self-offloading, V2V offloading, general user preference, individual UV preference, and the peak time change of content preference on the design of the caching strategy. Therefore, it was also confirmed that the network data offloading performance could be effectively improved by rationally designing the caching strategy between UVs and making full use of the self-caching capability. Anjum et al. [17] proposed a cache method based on two-tiered segment, which divided the storage capacity of each mobile device into two areas. Their research could effectively reduce the startup and playback delay of video in the network. Ma et al. [18] investigated the application of the cluster center caching strategy in data sharing, and analyzed the effectiveness of the cluster center caching strategy by using network coverage probability, average completion ratio, and cache hit ratio. Lee et al. [19] studied the optimal caching strategy and cooperative distance design of V2V caching network from the aspects of network throughput and EE. Cai et al. [20] proposed a social-aware mobile edge caching strategy based on network coding, considering the impact of location proximity and UV social relations on caching strategies. S. Sinem Kafıloğlu et al. [21] proposed two cooperative cache replacement algorithms based on distance and priority classification to optimize network energy consumption. Because the battery capacity of each UV was limited, Li et al. [22] studied the design of caching strategy for V2V-assisted wireless networks from the perspective of network offloading gain and energy consumption. The above researches have made important contributions from various perspectives based on V2V wireless caching networks, but they all ignore the communication security issues in MEC-enabled air-to-ground integrated IoV.

In the era of advanced network technology, the use of various applications generates a large amount of unknown personal privacy data. Once the personal privacy data is leaked, it can seriously affect the privacy of UVs and even the safety of UVs' property and life. Therefore, people's privacy and security problems in MEC-enabled air-to-ground integrated IoV must be paid great attention to. Physical layer security [23,24] and wireless caching can be easily integrated in a low complexity and high flexibility manner, mainly including two reasons: (1) Physical layer security achieves wireless secrecy by using eavesdropping channel coding, which is different from source encryption. This encryption method can enable the cached files to be reused, thereby improving the reuse probability of the content in the edge cache. (2) Physical layer security can exploit the inherent randomness of wireless channels without necessarily relying on keys. The security problem in wireless networks is gradually attracting researchers' attention. Refs. [25–28] have done some research on the security problem of random wireless networks, but the research on using physical layer security to ensure that file transmissions in edge cache are not eavesdropped is still rare. There even lacks a basic theoretical security performance analysis framework and optimization from the perspective of random geometry. Wang and Zheng [25] investigated the physical layer security of random cellular networks, which laid the foundation for the study of wireless network security. Liu et al. [26] derived the exact expression of outage probability of large-scale access to wireless networks through physical layer security. Zheng et al. [27] studied the joint design of small cell network-based cache placement and physical layer transmission in the presence of randomly distributed eavesdroppers to improve the secure content delivery probability of small cell networks. Ren et al. [28]

proposed a mobile-aware cooperative coding caching strategy for the high-speed mobility of users and the secure transmission of content. Inspired by the above researches, this paper focuses on the research of security problems in the MEC-enabled air-to-ground integrated IoV to prevent the important data of UVs from being forged or tampered by attackers and provide a strong guarantee for UVs' privacy.

In this paper, we mainly investigate the cache strategy design and physical layer security in the MEC-enabled air-to-ground integrated IoV to improve the data offloading performance and the anti-eavesdropping capability. The main work and achievements are described as follows

- We propose a novel mobile edge cache strategy based on physical layer security, which enhances the adjacent discovery capability of files and improves the probability of secure transmission. Based on random geometry theory, we calculate the precise expression of the MEC-enabled air-to-ground integrated IoV security offloading ratio. Taking the security offloading ratio as the objective function, we build a joint optimization problem about the cache strategy and the secure transmission rate;
- Since the cache strategy and the secure transmission rate are tightly coupled in the objective function, it is difficult to directly obtain the joint optimal solution. Therefore, we propose an alternating optimization algorithm, which can obtain the joint optimal solution of the cache strategies and the secure transmission rate to maximize the network security offloading ratio;
- Through a numerical simulation of the key technical parameters, the results show that the network security offloading performance of the proposed caching strategy is superior to the existing caching strategies.

Other sections of the paper are arranged as follows. Section 2 is the air-to-ground integrated IoV system model, and Section 3 shows the problem formulation and analysis. The cache strategy optimization problem is presented in Section 4. In Section 5, theoretical analysis and numerical simulation results are described. Finally, the conclusions of this paper are drawn in Section 6.

2. System Model

This section mainly introduces the MEC-enabled air-to-ground integrated IoV network model and file access model considered in our research content.

2.1. Network Model

In this paper, we consider a MEC-enabled air-to-ground integrated IoV model, in which cooperative vehicles (CVs), RVs and eavesdropping vehicles (EVs) are modeled as a homogeneous Poisson point process (HPPP) [29] with density λ_p, λ_r and λ_e, respectively, as shown in Figure 1. This is a small cell network, such as a single road or an intersection of two roads. In this case, we can model network nodes into Poisson point process and use random geometric theory analysis. The PPP model is usually more accurate for the vehicle network formed on this sparse road layout [30–33]. Each UV has a single antenna with transmission power P_t. For large-scale fading we consider a standard fading model $r^{-\alpha}$. r represents the communication distance between UVs, α is the fading factor and $\alpha > 2$ is the pre-condition. For small-scale fading, we consider Rayleigh fading, in which the channel gain follows the exponential distribution with unit mean independently, i.e., $G \sim \exp(1)$ [34,35]. The reason is that this work focuses on Highrise Urban scenarios, consisting of many ground obstructions. Therefore, traditional air-to-ground channels (e.g., Nakagami fading channels [36,37]) may not be suitable for our considered scenarios. This assumption has been widely used for vehicular communications [38,39]. If the UV caches the required files in their own storage space, the UV can get it directly without consuming other resources. Otherwise, the required files will be obtained through cooperation between UVs. We assume that the ABS caches all files and knows all UV information to coordinate V2V cooperative communication.

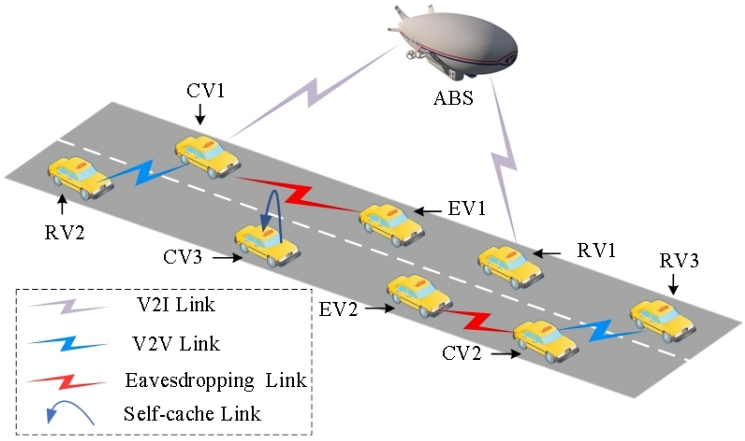

Figure 1. MEC-enabled air-to-ground integrated IoV model.

We consider a limited file library $\mathcal{F} = \{1, 2, \cdots, F\}$, where 1-st is the most popular file. Each CV has a limited cache capacity S ($S << F$). Due to the size and cost constraints assumptions in Refs. [22,40], we assume that each CV can cache one file, which easily generalizes to the multiple file case. We assume that each UV can obtain the file independently, which obeys the Zipf distribution [41]. The probability that the $f-th$ file is requested by the UE can be expressed as $p_f = f^{-\varepsilon}/\sum_{i=1}^{F} i^{-\varepsilon}$, where ε is the popularity factor. Each CV can cache files according to optimized cache strategy $\mathbf{q} = \left\{q_1, \cdots, q_f, \cdots, q_F\right\}$, where q_f represents the probability that the $f-th$ file is cached. Based on the thinning property [42], the location of the CV that cached file f follows a HPPP distribution with density $q_f \lambda_p$.

2.2. File Access Model

We consider that the ABS caches all files and knows the RVs' request information and the CVs' cache status. The ABS will schedule the content according to the known information. If the requester sends the file request information, there are two ways to obtain the files, namely self-cache and V2V cache. When self-cache and V2V caching fail, the ABS provides the required files to the RV.

- **Case 1: self-cache:** If the RV caches the desired file in the local cache, and the RV will get the desired file directly from the local cache without associating other CVs. This is a special case consideration in edge caching, which is often ignored in existing related researches [43–45];
- **Case 2: V2V cache:** If the RV does not cache the required file in the self-cache, then the RV will obtain the required file from surrounding CVs through V2V communication. This process involves the successful establishment of V2V communication and the secure transmission of files. The research will be discussed in later chapters.

3. Problem Formulation and Analysis

In this section, we mainly analyze the data offloading performance of the MEC-enabled air-to-ground integrated IoV, and take the network security offloading ratio as the main quantitative indicator. The network security offloading ratio is defined as the probability that a file is successfully found around the RV and transmitted confidentially at a given data rate threshold. Therefore, the total network security offloading ratio of the MEC-enabled air-to-ground integrated IoV H_{total} is defined as

$$H_{total} = \sum_{f=1}^{F} p_f (P_s + P_{V2V} D_s D_c), \tag{1}$$

where P_s and P_{V2V} are the self-cache data offload ratio and the probability that V2V successfully finds the file, respectively. D_s and D_c are the probability of successful V2V connection and the probability of secure transmission, respectively.

3.1. Self-Cache Offloading Ratio

We calculate the probability that the RV finds the required file in the local cache library as the self-cache offloading ratio. Therefore, the self-cache data offloading ratio can be calculated as

$$P_s = \sum_{f=1}^{F} p_f q_f. \tag{2}$$

3.2. V2V Cache Offloading Ratio

If the RV cannot obtain the required files through self-caching, then the V2V cache needs to be enabled to obtain the required files from neighboring CVs. We assume that CV_1 caches the file f, because the location of CV_1 follows a HPPP distribution, so the probability density function of the RV and CV_1 with association distance r is calculated as $f = 2\pi q_f \lambda_p r e^{-\pi q_f \lambda_p r^2}$ [46]. Therefore, the probability that the RV successfully sensing the file f within the communication range z can be calculated as

$$P_{V2V,f} = \Big(1 - q_f\Big)(1 - e^{-\pi q_f \lambda_p z^2}). \tag{3}$$

From Equation (3), we can calculate the probability that the RV successfully sensing all files in the file library $\mathcal{F} = \{1, 2, \cdots, F\}$ as

$$P_{V2V} = \sum_{f=1}^{F} p_f \Big(1 - q_f\Big)(1 - e^{-\pi q_f \lambda_p z^2}). \tag{4}$$

Based on Shannon's theorem, when the transmission capacity C_b between UVs is $C_b \geq R_s + R_v$, the V2V communication can be successfully established. When EV's channel capacity C_e is $C_e \leq R_v$, the communication can be transmitted confidentially, where R_s and R_v represent the original transmission rate and redundant transmission rate, respectively. Therefore, the successful connection probability and security transmission probability of the cache-enabled V2V communication can be calculated as $D_s = \mathbb{P}\{\log_2(1 + SINR_b) \geq R_s + R_v\}$ and $D_c = \mathbb{P}\{\log_2(1 + SINR_e) \leq R_v\}$. Specifically, $SINR_b = \frac{P_t g_{b,0} r_{b,0}^{-\alpha}}{I_b + N_0 w_1}$ is the signal-to-interference-and-noise ratio (SINR) at RV, where I_b represents the interference generated by surrounding the RVs, whose location obeys a HPPP Φ_1 with density $\lambda_r P_{D2D}$. $N_0 w_1$ is the noise power at the receiver, $g_{b,0}$ is the channel gain, and $r_{b,0}$ represents the cooperation distance between UVs. $SINR_e = \frac{P_t g_{e,0} r_{e,0}^{-\alpha}}{I_e + N_0 w_2}$ is the SINR at EV, where $r_{e,0}$ is the distance between the CV and the EV, $g_{e,0}$ is the channel gain. The random variable $I_e = \sum_{i \in \Phi_2 \setminus \mathrm{CP}_0} P_t g_i r_i^{-\alpha}$ refers to the interference of EVs around, and $N_0 w_2$ represents the received noise power. We do further calculations of probabilities D_s and D_c, the expression can be rewritten as

$$\begin{aligned} D_s &= \mathbb{P}\left\{\log_2\left(1 + \frac{P_t g_{b,0} r_{b,0}^{-\alpha}}{I_b + N_0 w_1}\right) \geq R_s + R_v\right\} \\ &\overset{(1)}{\approx} \mathbb{P}\left\{g_{b,0} \geq I_b P_t^{-1} r_{b,0}^{\alpha} 2^{R_s + R_v}\right\} \overset{(2)}{=} \mathbb{E}_{I_b}\left(e^{-I_b P_t^{-1} r_{b,0}^{\alpha} 2^{R_s + R_v}}\right), \\ &\overset{(2)}{=} \mathcal{L}_{I_b}\left(P_t^{-1} r_{b,0}^{\alpha} 2^{R_s + R_v}\right) \end{aligned} \tag{5}$$

where step (1) considers the interference restriction between UVs, step (2) considers small-scale fading that follows an exponential distribution $g_{b,0} \sim \exp(1)$ [34,35], and step (3)

is the Laplace transform of the random variable I_b [47,48], where $I_b = \sum_{i\in\Phi_1\setminus \mathrm{CP}_0} P_t g_i r_i^{-\alpha}$. The Laplace transform of the random variable I_b can be calculated as

$$\begin{aligned}
\mathcal{L}_{I_b}(s) &= \mathbb{E}_{\Phi_1, g_i}\left(e^{-s\sum_{i\in\Phi_1\setminus \mathrm{CP}_0} P_t g_i r_i^{-\alpha}}\right) \\
&= \mathbb{E}_{\Phi_1, g_i}\left[\prod_{i\in\Phi_1\setminus \mathrm{CP}_0}\left(1+sP_t r_i^{-\alpha}\right)^{-1}\right] \\
&= \exp\left[-2\pi\lambda_r P_{V2V}\int_0^{\infty}\left(1-\frac{1}{1+sP_t x^{-\alpha}}\right)x dx\right] \\
&= \exp\left\{-2\pi\lambda_r P_{V2V}\int_0^{\infty}\left[1-\frac{x}{1+(sP_t)^{-1}x^{\alpha}}\right]dx\right\}, \\
&= \exp\left(-2\pi\lambda_r P_{V2V}\int_0^{\infty}\frac{y^{\frac{2}{\alpha}-1}}{1+(sP_t)^{-1}y}\frac{1}{\alpha}dy\right) \\
&\overset{(1)}{=} \exp\left[-2\pi^2\lambda_r P_{V2V}(sP_t)^{\frac{2}{\alpha}}\csc\left(\frac{2}{\alpha}\right)\alpha^{-1}\right]
\end{aligned} \tag{6}$$

where step (1) is obtained by (Ref. [49] Equation (3.194.4)) when the path loss factor satisfies $\alpha > 2$. Then, by substituting $s = P_t^{-1} r_{b,0}^{\alpha} 2^{R_s+R_v}$ into Equation (6) we can rewrite Equation (5) as

$$\begin{aligned}
D_s &= \mathcal{L}_{I_b}\left(P_t^{-1} r_{b,0}^{\alpha} 2^{R_s+R_v}\right) \\
&= \exp\left[-2\pi^2\lambda_r P_{V2V} 2^{2(R_s+R_v)/\alpha}\csc\left(2\pi\alpha^{-1}\right)\alpha^{-1} r_{b,0}^2\right].
\end{aligned} \tag{7}$$

Furthermore, we calculate the secure transmission probability of the MEC-enabled air-to-ground integrated IoV D_c. The SINR of EV can be expressed as $SINR_e = \frac{P_t g_{e,0} r_{e,0}^{-\alpha}}{I_e + N_0 w_2}$. The position at EVs follow a HPPP distribution Φ_2 with density λ_e. Therefore, the secure transmission probability D_c can be recalculated as

$$\begin{aligned}
D_c &= \mathbb{P}\{\log_2(1+SINR_e) \le R_v\} \\
&= \mathbb{P}\left\{\log_2\left(1+\frac{P_t g_{e,0} r_{e,0}^{-\alpha}}{I_e + N_0 w_2}\right) \le R_v\right\} \\
&= \mathbb{P}\left\{g_{e,0} \le I_e P_t^{-1} r_{e,0}^{\alpha} 2^{R_v}\right\} = 1 - \mathbb{P}\left\{g_{e,0} > I_e P_t^{-1} r_{e,0}^{\alpha} 2^{R_v}\right\} \\
&= 1 - \mathbb{E}_{I_e}\left(e^{-I_e P_t^{-1} r_{e,0}^{\alpha} 2^{R_v}}\right) = 1 - \mathcal{L}_{I_e}\left(P_t^{-1} r_{e,0}^{\alpha} 2^{R_v}\right)
\end{aligned}. \tag{8}$$

Then, we do the Laplace transform of the random variable I_e in Equation (8). The calculation process is as follows

$$\begin{aligned}
\mathcal{L}_{I_e}\left(P_t^{-1} r_{e,0}^{\alpha} 2^{R_v}\right) &= \mathbb{E}_{\Phi_2, g_i}\left(e^{-s\sum_{i\in\Phi_2\setminus \mathrm{CP}_0} P_t g_i r_i^{-\alpha}}\right) \\
&= \mathbb{E}_{\Phi_2, g_i}\left[\prod_{i\in\Phi_2\setminus \mathrm{CP}_0}\left(1+r_{e,0}^{\alpha} 2^{R_v} r_i^{-\alpha}\right)^{-1}\right] \\
&= \exp\left[-2\pi\lambda_e\int_0^{\infty}\left(1-\frac{1}{1+r_{e,0}^{\alpha} 2^{R_v} x^{-\alpha}}\right)x dx\right]. \\
&= \exp\left(-2\pi\lambda_e\int_0^{\infty}\frac{y^{\frac{2}{\alpha}-1}}{1+\left(r_{e,0}^{\alpha} 2^{R_v}\right)^{-1} y}\frac{1}{\alpha}dy\right) \\
&= \exp\left[-2\pi^2\lambda_e 2^{2R_v/\alpha}\csc\left(2\pi\alpha^{-1}\right)\alpha^{-1} r_{e,0}^2\right]
\end{aligned} \tag{9}$$

Therefore, through the calculation of Equations (8) and (9), we can get the expression of the secure transmission probability D_c as

$$D_c = 1 - \exp\left[-2\pi^2\lambda_e 2^{2R_v/\alpha}\ \csc\left(2\pi\alpha^{-1}\right)\alpha^{-1}r_{e,0}^2\right]. \tag{10}$$

Finally, by substituting Equations (2), (3), (7) and (10) into Equation (1), we can get a closed-form expression for the security offloading ratio of the MEC-enabled air-to-ground integrated IoV as

$$H_{total} = \sum_{f=1}^{F} p_f\left\{q_f + \left(1 - q_f\right)(1 - e^{-\pi q_f \lambda_p z^2})D_s D_c\right\}. \tag{11}$$

4. The Cache Strategy and Secure Transmission Rate Optimization Problem

In this section, we investigate the joint effect of caching strategy and the secure transmission rate on the security offloading ratio of MEC-enabled air-to-ground integrated IoV. The redundancy rate and content cache probability are jointly optimized to maximize the network security offload probability. We study the optimal trade-off between file sharing and privacy security. According to the theoretical derivation results of the Section 3, we can construct the joint optimization as

$$\mathbf{P1}: \max_{\mathbf{q}, R_v} H_{total} \tag{12a}$$

$$s.t. \sum_{f=1}^{F} q_f \le S \tag{12b}$$

$$0 \le q_f \le 1 \tag{12c}$$

$$R_v \ge 0 \tag{12d}$$

where the objective function (12a) represents the probability that the requester finds the desired file and obtains it successfully in the MEC-enabled air-to-ground integrated IoV. Constraint (12b) indicates that the cache capacity of each CV is limited. Constraint (12c) is the cache probability of each file. Constraint (12d) ensures that the secure transmission rate of the file is positive.

Due to the complexity brought by the exponential term in the objective function H_{total}, the joint optimization problem **P1** is an NP-hard problem [50]. It is difficult for us to directly obtain the joint optimal solution. From the objective function H_{total} we can observe that if the security transmission rate is increased, the probability of the successful V2V connection will decrease. Conversely, if the security transmission rate is too small, the security transmission probability will be reduced. Therefore, there may be an optimal secure transmission rate to maximize the security offloading ratio of the MEC-enabled air-to-ground integrated IoV. Furthermore, the caching strategy and the secure transmission rate are tightly coupled, so each caching strategy may correspond to an optimal secure transmission rate. Therefore, we propose an alternating joint optimization method. First, we transform the original problem **P1** into two sub-problems ($\mathbf{P1}-\mathbf{a}$ and $\mathbf{P1}-\mathbf{b}$) for independent optimization, and then propose a joint optimization algorithm, which can finally solve the optimal solution of the joint cache strategy and the secure transmission rate.

4.1. Optimal Secure Transmission Rate for a Given Cache Strategy

In this subsection, our work focuses on optimizing the secure transmission rate of the MEC-enabled air-to-ground integrated IoV under a given caching strategy. Therefore, the sub-optimization problem is defined as

$$\begin{aligned} &\mathbf{P1}-\mathbf{a}: \max_{R_v} H_{total} \\ &s.t.\ \ R_v \ge 0 \end{aligned} \tag{13}$$

In order to get the optimal solution of the secure transmission rate R_v, we must first judge the Hessian matrix of of the objective function H_{total}. The first derivative of H_{total} can be solved as

$$\begin{aligned}\frac{\partial H_{total}}{\partial R_v} &= \sum_{f=1}^{F} p_f \left[q_f + \left(1 - q_f\right) P_{V2V} \frac{\partial D_s D_c}{\partial R_v} \right] \\ &= \sum_{f=1}^{F} p_f \left[q_f + \left(1 - q_f\right) P_{V2V} \left(\frac{\partial D_s}{\partial R_v} \cdot D_c + \frac{\partial D_c}{\partial R_v} \cdot D_s \right) \right]\end{aligned}. \tag{14}$$

For simplicity, we set $\varphi_b = 2\pi^2 \lambda_r \csc\left(2\pi\alpha^{-1}\right)\alpha^{-1} r_{b,0}^2 2^{2R_s/\alpha}$ and $\varphi_e = 2\pi^2\lambda_e \csc\left(2\pi\alpha^{-1}\right)\alpha^{-1} r_{e,0}^2$. So D_s and D_c are rewritten as $D_s = \exp\left(-k_b P_{V2V} 2^{2R_v/\alpha}\right)$, and $D_c = 1 - \exp\left(-k_e 2^{2R_v/\alpha}\right)$. The first derivative of D_s and D_c with respect to R_v can be calculated as

$$\frac{\partial D_s}{\partial R_v} = -\frac{2}{\alpha} k_b P_{V2V} \exp\left(-k_b P_{V2V} 2^{2R_v/\alpha}\right) 2^{2R_v/\alpha} \ln 2. \tag{15}$$

$$\frac{\partial D_c}{\partial R_v} = \frac{2}{\alpha} k_e \exp\left(-k_e 2^{2R_v/\alpha}\right) 2^{2R_v/\alpha} \ln 2. \tag{16}$$

By substituting Equations (15) and (16) into Equation (14) , we can further rewrite $\frac{\partial H_{total}}{\partial R_v}$ as

$$\begin{aligned}\frac{\partial H_{total}}{\partial R_v} &= \sum_{f=1}^{F} p_f \left[q_f + \left(1 - q_f\right) P_{V2V} \frac{\partial D_s D_c}{\partial R_v} \right] \\ &= \sum_{f=1}^{F} p_f \left\{ \begin{array}{l} q_f + \left(1 - q_f\right) P_{V2V} \frac{2}{\alpha} 2^{2R_v/\alpha} \ln 2 \exp\left(-k_b P_{V2V} 2^{2R_v/\alpha}\right) \\ \times \left[-k_b P_{V2V} + \left(k_b P_{V2V} + k_e\right) \exp\left(-k_e 2^{2R_v/\alpha}\right) \right] \end{array} \right\}\end{aligned}. \tag{17}$$

By analyzing Equation (17), it can be seen that $\left(1 - q_f\right) \exp\left(-k_b P_{V2V} 2^{2R_v/\alpha}\right) \ln 2 \times P_{V2V} \frac{2}{\alpha} 2^{2R_v/\alpha}$ is a positive term, so the positive or negative of $\frac{\partial H_{total}}{\partial R_v}$ is determined by $\vartheta\left(q_f\right) = -k_b P_{V2V} + \left(k_b P_{V2V} + k_e\right) \exp\left(-k_e 2^{2R_v/\alpha}\right)$. Obviously $\vartheta\left(q_f\right)$ belongs to the exponential function. So according to the properties of the exponential function, $\vartheta\left(q_f\right)$ is a monotonically decreasing function. Therefore, we set $\vartheta\left(q_f\right)$ equal to 0 to get the extreme point R_v^* of the function H_{total}, which is calculated as

$$R_v^* = \frac{\alpha}{2} \log_2 \left\{ -\frac{\ln[\varphi_b P_{V2V} / (\varphi_b P_{V2V} + \varphi_e)\,]}{\varphi_e} \right\}. \tag{18}$$

This means that $\frac{\partial H_{total}}{\partial R_v}$ is positive within the interval of $0 < R_v < R_v^*$ and negative within $R_v > R_v^*$. Thus, it can be determined that H_{total} is a concave function within the interval $R_v > 0$, and the maximum point is R_v^*. We can optimize R_v^* by a fixed $\mathbf{q}$.

4.2. Optimal Cache Strategy for a Given Secure Transmission Rate

In this subsection, we optimize the cache strategy based on the given secure transmission rate. The sub-problem with respect to cache strategy $\mathbf{q} = \left\{ q_1, \cdots, q_f, \cdots, q_F \right\}$ is formulated as

$$\begin{aligned} \mathbf{P1}-\mathbf{b}: \max_{\mathbf{q}} & H_{total} \\ s.t. & \sum_{f=1}^{F} q_f \leq C \\ & 0 \leq q_f \leq 1 \end{aligned} \tag{19}$$

Proposition 1. *The proposed optimization problem* $\mathbf{P1}-\mathbf{b}$ *is a convex optimization problem with regard to* $0 \leq q_f \leq 1$.

Proof of Proposition 1. See Appendix A. □

Through Proposition 1, we know that the optimization problem $\mathbf{P1}-\mathbf{b}$ about the caching strategy is a convex programming problem. Generally, the optimization problem $\mathbf{P1}-\mathbf{b}$ can obtain the closed expression of the optimal cache strategy $\mathbf{q}^*$ through the analytical method, but the complex structure introduced by the exponential term in the objective function H_{total} and the existence of inequality constraints make it difficult for the optimization problem $\mathbf{P1}-\mathbf{b}$ to obtain the closed expression of the optimal cache strategy $\mathbf{q}^*$. Therefore, we use the *fmincon* module of MATLAB to solve the optimization problem $\mathbf{P1}-\mathbf{b}$ [19,51,52]. It can ensure that the constrained optimization problem $\mathbf{P1}-\mathbf{b}$ converges to the global optimal solution.

4.3. Iterative Algorithm for Joint Optimization

In this section, we jointly optimize the caching strategy $\mathbf{q}$ and the secure transmission rate R_v to maximize the security offloading rate of the MEC-enabled air-to-ground integrated IoV. From the previous theoretical analysis, it can be seen that the cache strategy $\mathbf{q}$ and the secure transmission rate R_v are the product relationship in the expression of the network security offloading ratio H_{total}, which makes the joint optimization more complicated. Therefore, we propose an alternating optimization algorithm to obtain the joint optimal solution of the caching strategy and the secure transmission rate. The details of the joint optimization algorithm are shown in Algorithm 1. In Algorithm 1, we first obtain the optimal secure transmission rate through a given caching strategy, and then solve the optimal caching strategy by obtaining the secure transmission rate, and alternately optimized each until the network security offloading ratio converges. Finally, a set of joint optimal solutions of the cache strategy $\mathbf{q}^*$ and the secure transmission rate R_v^* are output.

Algorithm 1 Joint optimization algorithm.

1: Initialize the cache strategy $\mathbf{q}$ to a feasible value.
2: **Repeat** Loop:
3: (a) Calculate the security transmission rate R_v by Equation (18).
4: (b) Update the file cache strategy $\mathbf{q}$ by solving the convex optimization problem $\mathbf{P1}-\mathbf{b}$ for fixed R_v.
5: (c) Update the secure transmission rate R_v in Equation (18) using the cache strategy solved in step (b).
6: **Until** the network security offloading ratio H_{total}, the optimal secure transmission rate R_v^* and the optimal cache strategy $\mathbf{q}^*$
7: Output H_{total}, R_v and $\mathbf{q}$

5. Simulation and Numerical Results

In this section, we use key technical parameters to verify the performance of the proposed caching strategy and the correctness of the theoretical analysis. To verify the security offload performance and cache efficiency performance of files, we compare the proposed caching strategy with the PAEH caching strategy [29] and the Uniform-baseline caching strategy [53]. The PAEH caching strategy considered the impact of the self-caching and the

successful transmission probability, which were the focus of current research in cooperative caching. By comparing the proposed cache strategy with the PAEH caching strategy, we can verify the security offloading ability of the proposed cache strategy. The uniform-baseline caching strategy is a cache strategy that does not consider the change of content popularity. This strategy, as the baseline cache strategy, appears in many related studies to prove the cache efficiency improvement ability of the proposed cache strategy. All the caching strategies consider the effect of self-caching. Unless otherwise specified, the simulation environment parameter settings in this paper are shown in Table 1.

Table 1. Simulation parameters.

Parameters	Value
Intensity of CVs λ_p	$4 \times 10^{-3}/\mathrm{m}^2$
Intensity of EVs λ_e	$2 \times 10^{-3}/\mathrm{m}^2$
V2V bandwidth W	20 MHz
Path loss exponent α	3.68
Noise power σ^2	-174 dBm/Hz
The number of files F	10 files
Each CV's cache capacity S	1 file
Zip parameter ε	0.6, 1

In Figure 2, we introduce the distribution probability of files under the proposed caching strategy, the PAEH caching strategy, and the uniform-baseline caching strategy. From Figure 2, we can easily see that the uniform-baseline caching strategy caches all files with the same probability. The proposed caching strategy and the PAEH caching strategy only cache a small number of high-ranked files. When the Zipf factor $\varepsilon = 1$, the proposed caching strategy and the PAEH caching strategy only need to cache the top 3 files to maximize the network security offloading rate, because an increase in the Zipf factor ε means that the probability of the file being requested becomes more concentrated. In order to increase the network security offload ratio, the proposed caching strategy and the PAEH caching strategy increase the caching probability of the top files. This is consistent with the high demand for a certain file in a certain period of time in the actual network. Lower-ranked files may not need to be cached due to the CV's limited cache capacity.

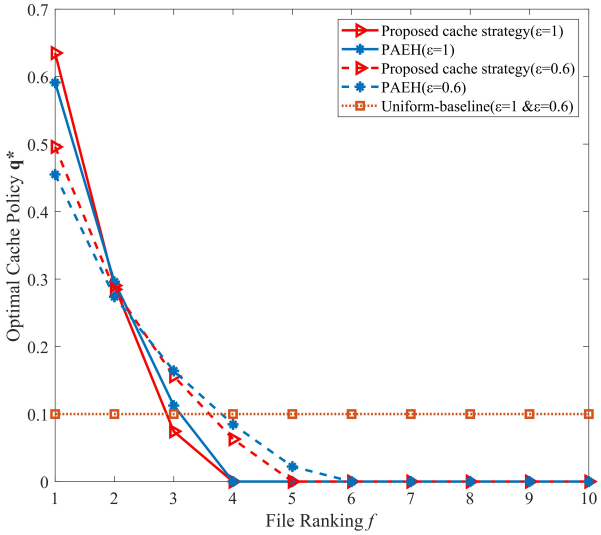

Figure 2. Distribution of caching strategies with different Zipf factors.

Figure 3 corresponds to optimization problem $\mathbf{P1}-\mathbf{a}$, which illustrates the optimization of the secure transmission rate for a given caching strategy. The specific values of the caching strategy adopted in Figure 3 are given in Table 2. As can be seen from Figure 3,

with the secure transmission rate increasing, the network security offloading ratio curve first increases to the extreme point and then drops rapidly. This phenomenon also verifies that our optimization scheme has an optimal solution. In addition, we can also observe that there is still the network security offloading ratio even when the secure transmission rate is zero, because the effect of self-caching is considered in our proposed caching strategy. We comprehensively take into account the factors of successful connection and security transmission of V2V communication in the proposed caching strategy. Therefore, under the condition of a very low secure transmission rate, the main way to obtain files by the proposed caching strategy may still be through self-caching. This may lead to the phenomenon that the curve starts. When the secure transmission rate is very low, the network security offloading ratio of the $\mathbf{q_1}$ cache strategy is lower than that of $\mathbf{q}_3$.

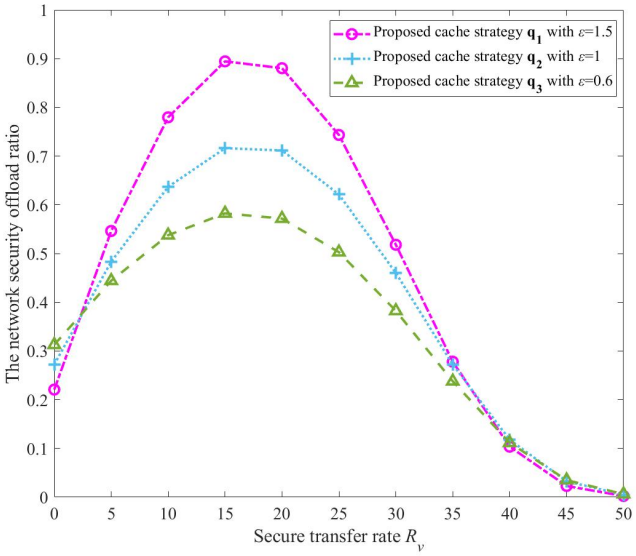

Figure 3. The curve of the network security offloading ratio versus the secure transmission rate.

Table 2. Three caching strategies adopted for Figure 3.

Zipf Parameters	Cache Probability of Files
$\mathbf{q_1}(\varepsilon = 1.5)$	0.7550 0.2450 0 0 0 0 0 0 0 0 0
$\mathbf{q}_2(\varepsilon = 1)$	0.6351 0.2904 0.0745 0 0 0 0 0 0 0 0
$\mathbf{q}_3(\varepsilon = 0.6)$	0.4960 0.2848 0.1562 0.0629 0 0 0 0 0 0 0

Figure 4 compares the proposed caching strategy, PAEH caching strategy and uniform-baseline caching strategy, with the increasing Zipf parameters. From Figure 4, we can easily see that the network security offloading ratio brought by the proposed caching strategy and PAEH caching strategy will increase rapidly with the increase of Zipf parameters. However, the network security offloading ratio of the uniform-baseline caching strategy is fixed on a horizontal line and does not change with the increase of the Zipf parameters. This result is the same as we expected, because the uniform-baseline caching strategy does not take into account the popularity of files, but caches all files with equal probability. Of course, the network security offloading ratio of the Uniform-baseline caching strategy is also the worst. Furthermore, we can also see that when the Zipf parameter is small, the proposed caching strategy is significantly better than the PAEH caching strategy, but the gap gradually decreases as the Zipf parameter increases. This is because the caching probability of our proposed scheme is strongly correlated with the probability of requesting files. The increase of popularity factor ε means that the probability of being requested for the most popular file increases. This will lead to the cache probability of the most popular file approaching 1,

and the cache probability of other files approaching 0. When the popularity factor ε gradually increases, both the proposed caching strategy and the PAEH caching strategy cache the top files, so the network security offloading ratio is gradually approaching.

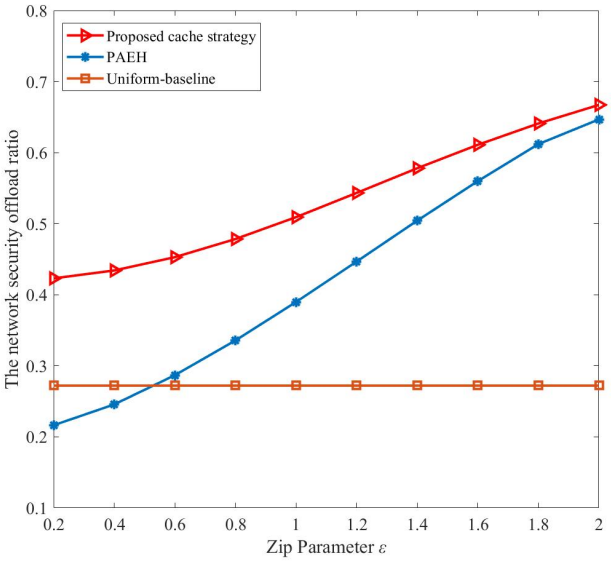

Figure 4. The network security offloading ratio of the caching strategies varies with Zipf parameters.

In Figure 5, we investigate the effect of different CV densities and EV densities ($\lambda_e = 1 \times 10^{-3}/m^2$, $\lambda_e = 4 \times 10^{-3}/m^2$, $\lambda_e = 10 \times 10^{-3}/m^2$) on the security offloading ratio of the MEC-enabled air-to-ground integrated IoV. Monte Carlo method is used to obtain the simulation results. From Figure 5, we can see that the simulation results match well with the theoretical values. This indicates that the theoretical derivation of this paper is reasonable. By analyzing the abscissa in Figure 5, we can conclude that the network security offloading ratio increases with the increase of CV density. This is because the increase in CV density also increases the probability of the RVs finding the surrounding required files. In addition, with the increase of CV density, the network security offloading ratio increases slowly and gradually tends to balance. This indicates that when the CV density reaches a certain value, the CV's cache capacity will become the main influencing factor of the network security offloading ratio. Furthermore, it can be seen from the three EV density curves that the network security offloading ratio decreases as the EV density increases. The reason for this phenomenon may be that the proposed caching strategy considers the factors of successful V2V communication connection and secure transmission. When the EV density increases, the risk of the file secure transmission also increases, which may lead to the decrease of the network security offloading ratio. In addition, with the increase in EV density, the network security offloading ratio will decrease slowly. The main reason is that the proposed caching strategy takes into account the impact of self-caching, which can ensure that the files can be obtained confidentially through self-caching even when the communication conditions are very risky.

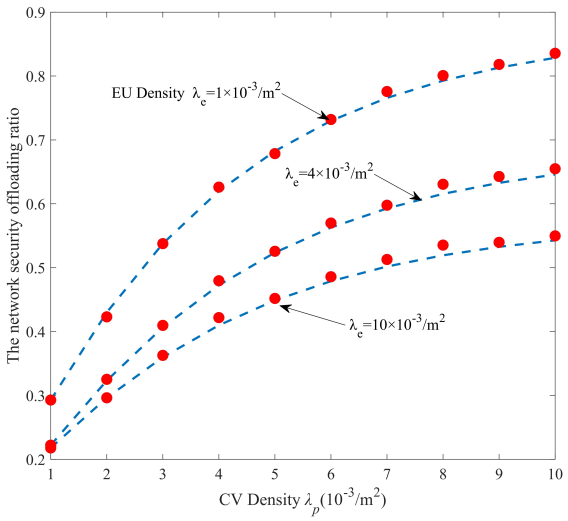

Figure 5. The network security offloading ratio varies with EV density and CV density.

In Figure 6, we compare the data security offloading performance of the proposed caching strategy, the PAEH strategy and the uniform-baseline caching strategy with different CV densities and Zipf parameters. It is obvious that all the caching strategies involved in the comparison will increase rapidly with the increase of CV density. The proposed caching strategy significantly outperforms the PAEH strategy and the uniform-baseline caching strategy in terms of the network security offloading ratio. This is the same conclusion as in Figure 5, in which the increase in the density of CV gives the requester a greater chance of obtaining the desired file. With the increase of Zipf parameters, the proposed caching strategy and the PAEH caching strategy will be significantly improved. Although both the proposed caching strategy and the PAEH caching strategy consider the influence of self-caching, it can be seen from the distribution of caching strategies in Figure 2 that the caching probability of the proposed caching strategy is strongly correlated with the request probability. However, the network security offloading ratio curves of the uniform-baseline caching strategy under the two Zipf parameters are coincident, because the uniform-baseline caching strategy does not consider the influence of content popularity.

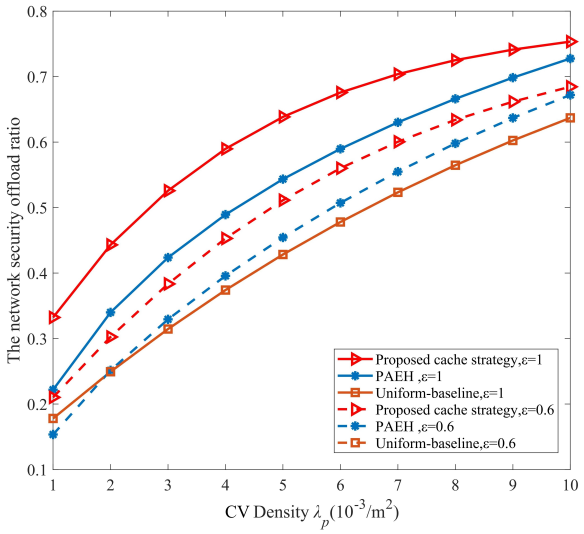

Figure 6. The network security offload ratio of different caching strategies varies with CV densities.

In Figure 7, we compare the network security offloading ratio of the proposed caching strategy, the PAEH strategy, and the uniform-baseline caching strategy under different

CV cache capacities. It can be seen from Figure 7 that the proposed caching strategy, the PAEH strategy, and the uniform-baseline caching strategy all increase with the increase of CV cache capacity. Due to the consideration of self-caching by all caching strategies and our assumption of a limited file library $F = 10$, when the CV cache capacity is $S = 10$, the network security offloading ratio of all caching strategies can reach the maximum value. In addition, we can also observe that with the increase of CV capacity, all cache strategies gradually narrow the gap in network security offloading ratio. Because when the cache capacity of the CV is large enough (compared with the file library), the probability that the requester obtains the required file through the self-cache is increased. At this time, the proportion of caching strategy and file popularity distribution to network data offloading will decrease. Therefore, the network security offloading ratio curve is gradually approaching. Furthermore, the proposed caching strategy is better than the PAEH strategy and the uniform-baseline caching strategy due to the consideration of the successful transmission of V2V communication. Since the uniform-baseline caching strategy does not fully utilize the cache space (all files are cached with the same probability), its network offloading ratio is the worst.

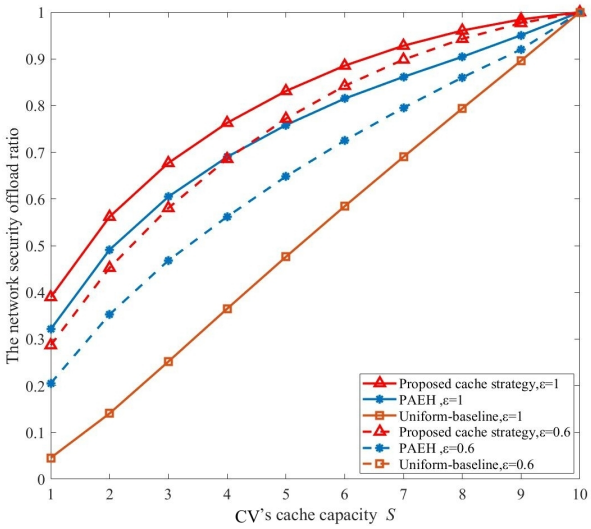

Figure 7. The network security offloading ratio of different caching strategies varies with CV cache capacity.

6. Conclusions

In this paper, we propose a novel mobile edge caching strategy to improve the security offloading ratio of the MEC-enabled air-to-ground integrated IoV, which comprehensively considers the effects of self-caching, the successful connection of V2V communication, and the secure transmission. On the basis of stochastic geometry theory and Laplace transform, we calculate the accurate expression for the network security offloading ratio. Based on the network security offloading ratio, we construct a joint optimization problem of the caching strategy and the secure transmission rate. Due to the complexity of the optimization problem, it is difficult to directly obtain the joint optimal solution of the caching strategy and the secure transmission rate. We propose an alternating optimization algorithm to jointly optimize the caching strategy and the secure transmission rate. Through the limited number of alternate optimizations, we can obtain a set of the optimal caching strategy and secure transmission rate that maximize the network security offloading ratio. Finally, we verify the superiority and feasibility of the proposed caching strategy through simulation experiments.

In addition, this paper focuses on considering a single line and a single ABS. If multiple lines and ABS are considered, road layout should be further considered. In this scenario, the network model should meet the Cox process or doubly stochastic Poisson point process.

However, the network will become more complicated, which is out of the scope of this paper and will be our future work. This paper focuses on highrise urban scenarios, consisting of many ground obstructions. Furthermore, studies regarding the comprehensive impact on LoS and NLoS groups will be conducted in the future.

Author Contributions: Methodology, Formal analysis, and Writing—Reviewing, W.W.; Supervision and Project administration, H.L.; Formal analysis, Y.L.; Project administration and Investigation, W.C.; Editing, R.L. All authors have read and agreed to the published version of the manuscript.

Funding: This work was supported by the National Natural Science Foundation of China (No. 62271395) and (No. 61401360), Natural Science Foundation of Shaanxi Province (No. 2021JM-076).

Institutional Review Board Statement: Not applicable.

Informed Consent Statement: Not applicable.

Data Availability Statement: Not applicable.

Conflicts of Interest: The authors declare no conflict of interest.

Appendix A

We set $\psi\left(q_f\right) = \exp\left(-k_b P_{V2V} 2^{2(R_s+R_v)/\alpha}\right) \times \left(1 - \exp\left(-k_e 2^{2R_v/\alpha}\right)\right)$, so the objective function can be rewritten as $H_{total} = \sum_{f=1}^{F} p_f\left[q_f + \left(1-q_f\right)(1-e^{-\pi q_f \lambda_p r^2})\psi\left(q_f\right)\right]$. The first derivative of H_{total} with respect to q_f can be calculated as

$$\begin{aligned}\frac{\partial H_{total}}{\partial q_f} &= 1 - (1-e^{-\pi q_f \lambda_p z^2})\psi\left(q_f\right) + \left(1-q_f\right)\psi\left(q_f\right) \\ &\quad \times \left[\pi\lambda_p r^2 e^{-\pi q_f \lambda_p r^2} - P_{V2V}{}' k_b 2^{2(R_s+R_v)/\alpha}\left(1-e^{-\pi q_f \lambda_p z^2}\right)\right]\end{aligned}. \tag{A1}$$

Furthermore, we can also calculate the second derivative of H_{total} with respect to q_f as

$$\begin{aligned}\frac{\partial^2 H_{total}}{\partial q_f^2} &= \psi\left(q_f\right)\left\{\begin{array}{l} -2\pi\lambda_p r^2 e^{-\pi q_f \lambda_p r^2} + 2P_{V2V}{}'\zeta\left(q_f\right) \\ +\left(1-q_f\right)\left[\begin{array}{l} -k_b 2^{2(R_s+R_v)/\alpha}\left(P_{V2V}{}'\right)^2\zeta\left(q_f\right) \\ -\left(\pi\lambda_p r^2\right)^2 e^{-\pi q_f \lambda_p r^2} - P_{V2V}{}''\zeta\left(q_f\right)\end{array}\right]\end{array}\right\}, \\ &= \psi\left(q_f\right)\left\{\begin{array}{l} -\left(1-q_f\right)\zeta\left(q_f\right)\left(P_{V2V}{}'\right)^2 k_b 2^{2(R_s+R_v)/\alpha} - \left(2+\left(1-q_f\right)\pi\lambda_p r^2\right)\pi\lambda_p r^2 e^{-\pi q_f \lambda_p r^2} \\ +k_b 2^{2(R_s+R_v)/\alpha}\left[2(1-e^{-\pi q_f \lambda_p z^2})P_{V2V}{}' - \left(1-e^{-\pi q_f \lambda_p r^2}\right)\left(1-q_f\right)P_{V2V}{}''\right]\end{array}\right\}\end{aligned} \tag{A2}$$

where $\zeta\left(q_f\right) = k_b 2^{2(R_s+R_v)/\alpha}\left(1-e^{-\pi q_f \lambda_p z^2}\right)$. Obviously, the other terms of $\partial^2 H_{total}/\partial q_f^2$ are negative, so we just need to judge the positive and negative of $G\left(q_f\right) = 2(1-e^{-\pi q_f \lambda_p z^2})P_{V2V}{}' - \left(1-e^{-\pi q_f \lambda_p r^2}\right)\left(1-q_f\right)P_{V2V}{}''$.The first derivative of $G\left(q_f\right)$ with respect to q_f can be calculated as

$$\begin{aligned}G\left(q_f\right)' &= 2\pi\lambda_p r^2 e^{-\pi q_f \lambda_p z^2} P_{V2V}{}' - \pi\lambda_p r^2 e^{-\pi q_f \lambda_p r^2}\left(1-q_f\right)P_{V2V}{}'' \\ &\quad - \left(1-e^{-\pi q_f \lambda_p r^2}\right)\left(1-q_f\right)P_{V2V}{}''' + 3(1-e^{-\pi q_f \lambda_p z^2})P_{V2V}{}'' \\ &= -(1-e^{-\pi q_f \lambda_p z^2})\pi\lambda_p r^2 e^{-\pi q_f \lambda_p r^2}\left[8 + 3\pi\lambda_p r^2\left(1-q_f\right)\right] \\ &\quad + 3(1-e^{-\pi q_f \lambda_p z^2})P_{V2V}{}''\end{aligned} \tag{A3}$$

Through the calculation of Equation (A4), we can easily judge the positive and negative of the second derivative $p_{V2V}{}''$.

$$p_{V2V}{}'' = -2\pi\lambda_p r^2 e^{-\pi q_f \lambda_p z^2} - \left(\pi\lambda_p r^2\right)^2 e^{-\pi q_f \lambda_p z^2}\left(1 - q_f\right) < 0. \tag{A4}$$

Therefore, we can get the conclusion $G\left(q_f\right)' < 0$, which represents $G\left(q_f\right)$ as a decreasing function within $0 \le q_f \le 1$. So, we can judge that the function $G\left(q_f\right) \le G(0) = 0$. Furthermore, we can get $\partial^2 H_{total}/\partial q_f^2 < 0$. Therefore, the objective function H_{total} is a concave function on the convex set $0 \le q_f \le 1$, then the optimization problem $\mathbf{P1} - \mathbf{b}$ is proved to be a standard convex optimization problem.

References

1. Cisco. *Cisco Annual Internet Report (2018–2023) White Paper*; Cisco: San Jose, CA, USA, 2020.
2. Israr, A.; Ali, Z.A.; Alkhammash, E.H.; Jussila, J.J. Optimization Methods Applied to Motion Planning of Unmanned Aerial Vehicles: A Review. *Drones* **2022**, *6*, 126. [CrossRef]
3. You, X.; Wang, C.X.; Huang, J.; Gao, X.; Zhang, Z.; Wang, M.; Huang, Y.; Zhang, C.; Jiang, Y.; Wang, J.; et al. Towards 6G wireless communication networks: Vision, enabling technologies, and new paradigm shifts. *Sci. China Inf. Sci.* **2021**, *64*, 1–74. [CrossRef]
4. Sun, W.; Li, S.; Zhang, Y. Edge caching in blockchain empowered 6G. *China Commun.* **2021**, *18*, 1–17. [CrossRef]
5. Wang, D.; Zhou, F.; Lin, W.; Ding, Z.; Al-Dhahir, N. Cooperative hybrid nonorthogonal multiple access-based mobile-edge computing in cognitive radio networks. *IEEE Trans. Cogn. Commun. Netw.* **2022**, *8*, 1104–1117. [CrossRef]
6. Wang, D.; Wu, M.; He, Y.; Pang, L.; Xu, Q.; Zhang, R. An HAP and UAVs Collaboration Framework for Uplink Secure Rate Maximization in NOMA-Enabled IoT Networks. *Remote Sens.* **2022**, *14*, 4501. [CrossRef]
7. He, Y.; Wang, D.; Huang, F.; Zhang, R.; Pan, J. Trajectory optimization and channel allocation for delay sensitive secure transmission in UAV-relayed VANETs. *IEEE Trans. Veh. Technol.* **2022**, *71*, 4512–4517. [CrossRef]
8. Thandavarayan, G.; Sepulcre, M.; Gozalvez, J. Generation of cooperative perception messages for connected and automated vehicles. *IEEE Trans. Veh. Technol.* **2020**, *69*, 16336–16341. [CrossRef]
9. Chen, Y.; Liu, Y.; Zhao, J.; Zhu, Q. Mobile edge cache strategy based on neural collaborative filtering. *IEEE Access* **2020**, *8*, 18475–18482. [CrossRef]
10. Wang, D.; He, T.; Zhou, F.; Cheng, J.; Zhang, R.; Wu, Q. Outage-driven link selection for secure buffer-aided networks. *Sci. China Inf. Sci.* **2022**, *65*, 1–6. [CrossRef]
11. He, Y.; Nie, L.; Guo, T.; Kaur, K.; Hassan, M.M.; Yu, K. A NOMA-enabled framework for relay deployment and network optimization in double-layer airborne access VANETs. *IEEE Trans. Intell. Transp. Syst.* **2022**, *23*, 22452–22466. [CrossRef]
12. He, Y.; Zhai, D.; Huang, F.; Wang, D.; Tang, X.; Zhang, R. Joint task offloading, resource allocation, and security assurance for mobile edge computing-enabled UAV-assisted VANETs. *Remote Sens.* **2021**, *13*, 1547. [CrossRef]
13. Grlj, C.G.; Krznar, N.; Pranjić, M. A Decade of UAV Docking Stations: A Brief Overview of Mobile and Fixed Landing Platforms. *Drones* **2022**, *6*, 17. [CrossRef]
14. Narang, M.; Xiang, S.; Liu, W.; Gutierrez, J.; Chiaraviglio, L.; Sathiaseelan, A.; Merwaday, A. UAV-assisted edge infrastructure for challenged networks. In Proceedings of the 2017 IEEE Conference on Computer Communications Workshops (INFOCOM WKSHPS), Atlanta, GA, USA, 1–4 May 2017; pp. 60–65.
15. Dai, Y.; Xu, D.; Maharjan, S.; Zhang, Y. Joint load balancing and offloading in vehicular edge computing and networks. *IEEE Internet Things J.* **2018**, *6*, 4377–4387. [CrossRef]
16. Ning, Z.; Zhang, K.; Wang, X.; Obaidat, M.S.; Guo, L.; Hu, X.; Hu, B.; Guo, Y.; Sadoun, B.; Kwok, R.Y. Joint computing and caching in 5G-envisioned Internet of vehicles: A deep reinforcement learning-based traffic control system. *IEEE Trans. Intell. Transp. Syst.* **2020**, *22*, 5201–5212. [CrossRef]
17. Anjum, N.; Yang, Z.; Khan, I.; Kiran, M.; Wu, F.; Rabie, K.; Bahaei, S.M. Efficient algorithms for cache-throughput analysis in cellular-d2d 5g networks. *Comput. Mater. Contin.* **2021**, *67*, 1759–1780. [CrossRef]
18. Ma, Z.; Nuermaimaiti, N.; Zhang, H.; Zhou, H.; Nallanathan, A. Deployment model and performance analysis of clustered D2D caching networks under cluster-centric caching strategy. *IEEE Trans. Commun.* **2020**, *68*, 4933–4945. [CrossRef]
19. Lee, M.C.; Molisch, A.F. Caching policy and cooperation distance design for base station-assisted wireless D2D caching networks: Throughput and energy efficiency optimization and tradeoff. *IEEE Trans. Wirel. Commun.* **2018**, *17*, 7500–7514. [CrossRef]
20. Cai, J.; Wu, X.; Liu, Y.; Luo, J.; Liao, L. Network coding-based socially-aware caching strategy in D2D. *IEEE Access* **2020**, *8*, 12784–12795. [CrossRef]
21. Kafıloğlu, S.S.; Gür, G.; Alagöz, F. Cooperative Caching and Video Characteristics in D2D Edge Networks. *IEEE Commun. Lett.* **2020**, *24*, 2647–2651. [CrossRef]
22. Li, M.; Cheng, N.; Gao, J.; Wang, Y.; Zhao, L.; Shen, X. Energy-efficient UAV-assisted mobile edge computing: Resource allocation and trajectory optimization. *IEEE Trans. Veh. Technol.* **2020**, *69*, 3424–3438. [CrossRef]

23. Wyner, A.D. The wire-tap channel. *Bell Syst. Tech. J.* **1975**, *54*, 1355–1387. [CrossRef]
24. Irram, F.; Ali, M.; Naeem, M.; Mumtaz, S. Physical layer security for beyond 5G/6G networks: Emerging technologies and future directions. *J. Netw. Comput. Appl.* **2022**, *206*, 103431. [CrossRef]
25. Wang, H.M.; Zheng, T.X. *Physical Layer Security in Random Cellular Networks*; Springer: Berlin/Heidelberg, Germany, 2016.
26. Liu, Y.; Qin, Z.; Elkashlan, M.; Gao, Y.; Hanzo, L. Enhancing the Physical Layer Security of Non-Orthogonal Multiple Access in Large-Scale Networks. *IEEE Trans. Wirel. Commun.* **2017**, *16*, 1656–1672. [CrossRef]
27. Zheng, T.X.; Wang, H.M.; Yuan, J. Physical-layer security in cache-enabled cooperative small cell networks against randomly distributed eavesdroppers. *IEEE Trans. Wirel. Commun.* **2018**, *17*, 5945–5958. [CrossRef]
28. Ren, D.; Gui, X.; Zhang, K.; Wu, J. Mobility-aware traffic offloading via cooperative coded edge caching. *IEEE Access* **2020**, *8*, 43427–43442. [CrossRef]
29. Meng, Y.; Zhang, Z.; Huang, Y. Cache-and energy harvesting-enabled d2d cellular network: Modeling, analysis and optimization. *IEEE Trans. Green Commun. Netw.* **2021**, *5*, 703–713. [CrossRef]
30. Farooq, M.J.; ElSawy, H.; Alouini, M.S. A stochastic geometry model for multi-hop highway vehicular communication. *IEEE Trans. Wirel. Commun.* **2015**, *15*, 2276–2291. [CrossRef]
31. Steinmetz, E.; Wildemeersch, M.; Quek, T.Q.; Wymeersch, H. A stochastic geometry model for vehicular communication near intersections. In Proceedings of the 2015 IEEE Globecom Workshops (GC Wkshps), San Diego, CA, USA, 6–10 December 2015; pp. 1–6.
32. Wu, Y.; Zheng, J. Modeling and Analysis of the Local Delay in an MEC-Based VANET for an Urban Area. *IEEE Trans. Veh. Technol.* **2022**, *71*, 13266–13280. [CrossRef]
33. Sial, M.N.; Deng, Y.; Ahmed, J.; Nallanathan, A.; Dohler, M. Stochastic geometry modeling of cellular V2X communication over shared channels. *IEEE Trans. Veh. Technol.* **2019**, *68*, 11873–11887. [CrossRef]
34. Andrews, J.G.; Baccelli, F.; Ganti, R.K. A tractable approach to coverage and rate in cellular networks. *IEEE Trans. Commun.* **2011**, *59*, 3122–3134. [CrossRef]
35. Chen, Z.; Pappas, N.; Kountouris, M. Probabilistic caching in wireless D2D networks: Cache hit optimal versus throughput optimal. *IEEE Commun. Lett.* **2017**, *21*, 584–587. [CrossRef]
36. Liu, H.W.; Zheng, T.X.; Wen, Y.; Feng, C.; Wang, H.M. Performance Analysis of Uplink mmWave Communications in C-V2X Networks. In Proceedings of the GLOBECOM 2020—2020 IEEE Global Communications Conference, Taipei, Taiwan, 7–11 December 2020; pp. 1–6.
37. Ullah, A.; Choi, W. Massive MIMO Assisted Aerial-Terrestrial Network: How Many UAVs Need to Be Deployed? *TechRxiv* **2022**, *10*, 36227.
38. Zhang, C.; Wei, Z.; Feng, Z.; Zhang, W. Spectrum sharing of drone networks. In *Handbook of Cognitive Radio*; Springer: Berlin/Heidelberg, Germany, 2019; pp. 1279–1304.
39. Zhang, S.; Zhu, Y.; Liu, J. Multi-UAV Enabled Aerial-Ground Integrated Networks: A Stochastic Geometry Analysis. *IEEE Trans. Commun.* **2022**, *70*, 7040–7054. [CrossRef]
40. Malak, D.; Al-Shalash, M. Device-to-device content distribution: Optimal caching strategies and performance bounds. In Proceedings of the 2015 IEEE International Conference on Communication Workshop (ICCW), London, UK, 8–12 June 2015; pp. 664–669.
41. Li, S.; Sun, W.; Zhang, H.; Zhang, Y. Physical Layer Security for Edge Caching in 6G Networks. In Proceedings of the GLOBECOM 2020—2020 IEEE Global Communications Conference, Taipei, Taiwan, 7–11 December 2020; pp. 1–6.
42. Stoyan, D.; Kendall, W.S.; Chiu, S.N.; Mecke, J. *Stochastic Geometry and Its Applications*; John Wiley & Sons: Hoboken, NJ, USA, 2013.
43. Chai, R.; Li, Y.; Chen, Q. Joint cache partitioning, content placement, and user association for D2D-enabled heterogeneous cellular networks. *IEEE Access* **2019**, *7*, 56642–56655. [CrossRef]
44. Vu, T.X.; Chatzinotas, S.; Ottersten, B.; Trinh, A.V. Full-duplex enabled mobile edge caching: From distributed to cooperative caching. *IEEE Trans. Wirel. Commun.* **2019**, *19*, 1141–1153. [CrossRef]
45. Mozaffari, M.; Saad, W.; Bennis, M.; Debbah, M. Unmanned aerial vehicle with underlaid device-to-device communications: Performance and tradeoffs. *IEEE Trans. Wirel. Commun.* **2016**, *15*, 3949–3963. [CrossRef]
46. Okabe, A.; Boots, B.; Sugihara, K.; Chiu, S.N. *Concepts and Applications of Voronoi Diagrams*; John Wiley: Chichester, UK, 2000.
47. Wang, C.; Li, Z.; Xia, X.G.; Shi, J.; Si, J.; Zou, Y. Physical layer security enhancement using artificial noise in cellular vehicle-to-everything (C-V2X) networks. *IEEE Trans. Veh. Technol.* **2020**, *69*, 15253–15268. [CrossRef]
48. Zheng, T.X.; Wen, Y.; Liu, H.W.; Ju, Y.; Wang, H.M.; Wong, K.K.; Yuan, J. Physical-Layer Security of Uplink mmWave Transmissions in Cellular V2X Networks. *IEEE Trans. Wirel. Commun.* **2022**, *21*, 9818–9833. [CrossRef]
49. Gradshteyn, I.S.; Ryzhik, I.M. *Table of Integrals, Series, and Products*; Academic Press: Cambridge, MA, USA, 2014.
50. Bai, T.; Wang, J.; Ren, Y.; Hanzo, L. Energy-efficient computation offloading for secure UAV-edge-computing systems. *IEEE Trans. Veh. Technol.* **2019**, *68*, 6074–6087. [CrossRef]
51. Su, Z.; Feng, W.; Tang, J.; Chen, Z.; Fu, Y.; Zhao, N.; Wong, K.K. Energy efficiency optimization for D2D communications underlaying UAV-assisted industrial IoT networks with SWIPT. *IEEE Internet Things J.* **2022**, *10*, 1990–2002. [CrossRef]

52. Boyd, S.; Boyd, S.P.; Vandenberghe, L. *Convex Optimization*; Cambridge University Press: Cambridge, UK, 2004.
53. Amer, R.; Baza, M.; Salman, T.; Butt, M.M.; Alhindi, A.; Marchetti, N. Optimizing joint probabilistic caching and channel access for clustered D2D networks. *J. Commun. Netw.* **2021**, *23*, 433–441. [CrossRef]